Politecnico di Torino

Porto Institutional Repository

[Article] Large-eddy simulation of hypersonic flows. Selective procedure to activate the sub-grid model wherever small scale turbulence is present

(Article begins on next page)

Selective large-eddy simulation of hypersonic flows. A new procedure to activate the filtering only in underresolved regions.

D.Tordella[a], M.Iovieno[a], S.Massaglia[b], A.Mignone[b]

[a]*Politecnico di Torino, Dipartimento di Ingegneria Aeronautica e Spaziale, Corso Duca degli Abruzzi 24, 10129 Torino, Italy*
[b]*Università di Torino, Dipartimento di Fisica Generale, via P.Giuria 1, 10129 Torino, Italy*

Abstract

We present the application of a new method for the localization of the regions where the turbulent fluctuations are underresolved to the *selective* large-eddy simulation (LES) of a compressible turbulent jet of Mach number equal to 5. The localization method is based on the introduction of a scalar probe function f which represents the magnitude of the *twisting-stretching* term normalized with the enstrophy [1]. The statistical analysis shows that, for a fully developed turbulent field of fluctuations, the probability that f is larger than 2 is zero, while, for an unresolved field, is finite. By computing f in each instantaneous realization of the simulation it is possible to locate the regions where the magnitude of the normalized stretching-twisting is anomalously high. This allows the identification of the regions where the subgrid model should be introduced into the governing equations (selective filtering). The results of the selective LES are compared with those of a standard LES, where the subgrid terms are used in the whole domain. The comparison is carried out by assuming as high order reference field a higher resolution Euler simulation of the compressible jet. It is shown that the *selective* LES modifies the dynamic properties of the flow to a lesser extent with respect to the classical LES.

1. Small scale detection criterion

In the large-eddy simulation (LES) of many flows, subgrid scales, that is fluctuations on a scale smaller than the grid size, are present only in part of the computational domain. In a recent paper [1] we have investigated the possibility to use a stretching based sensor for the detection of underresolved regions

in large-eddy simulations of turbulent flows. The criterion is based on the introduction of a local functional of vorticity and velocity gradients: the regions where the fluctuations are unresolved are located by means of the scalar probe function [1]

$$f(\mathbf{u}, \boldsymbol{\omega}) = \frac{\mid (\boldsymbol{\omega} - \overline{\boldsymbol{\omega}}) \cdot \nabla(\mathbf{u} - \overline{\mathbf{u}}) \mid}{\mid \boldsymbol{\omega} - \overline{\boldsymbol{\omega}} \mid^2} \tag{1}$$

where $\mathbf{u}$ is the velocity vector, $\boldsymbol{\omega} = \nabla \times \mathbf{u}$ is the vorticity vector and the overbar indicates the statistical average. Function (1) is a normalized scalar form of the vortex-stretching term that represents the inertial generation of three dimensional vortical small scales. When the flow is three dimensional and rich in small scales f is necessarily different from zero, while, on the other hand, it is instead equal to zero in a two-dimensional vortical flow. The mean flow is subtracted from the velocity and vorticity fields in order to consider the fluctuating part only of the field. A priori test of the spatial distribution of functional test have been performed by computing the statistical distribution of f in a fully resolved turbulent fluctuation field (DNS of a homogeneous and isotropic turbulent flow (1024^3, $Re_\lambda = 230$, data from [2])) and in some unresolved instances obtained by filtering this DNS field on coarser grids (from 512^3 to 64^3).

It has been shown [1] that shows that the probability that f assumes values larger than a given threshold t_ω is always higher in the filtered fields and increases when the resolution is reduced. The difference between the probabilities in fully resolved and in filtered turbulence is maximum when t_ω is in the range $[0.4, 0.5]$ for all resolutions. In such a range the probability $p(f \geq t_\omega)$ that f is larger than t_ω in the less resolved field is about twice the probability in the DNS field. Furthermore, beyond this range this probability normalized over that of resolved DNS fields it is gradually increasing becoming infinitely larger. From that it is possible to introduce a threshold t_ω of the values of f, such that, when f assumes larger values the field could be considered locally unresolved and should benefit from the local activation of the Large Eddy Simulation method (LES) by inserting a subgrid scale term in the motion equation. The values of this threshold is arbitrary, as there is no sharp cut, but it can be reasonably chosen to be equal to that where the difference between the resolved and unresolved field is maximum, that is $t_\omega \approx 0.4$.

Such value of the threshold has been used to investigate the presence of

2

regions with anomalously high values of the functional f, by performing a set of a priori tests on existing Euler simulations of the temporal evolution of a perturbed cylindrical hypersonic light jet with an initial mach number equal to 5 and ten times lighter than the surrounding external ambient [1]. When the effect of the introduction of subgrid scale terms in the transport equation is extrapolated from those a priori tests, they positively compare with experimental results and show the convenience of the use of such a procedure [1, 12].

In this paper we have carried out large-eddy simulations of the same temporal evolving jet, where the subgrid terms are selectively introduced in the transport equations by means of the local stretching criterion [1]. The aim is not to model a specific jet, but instead we want to understand, from a physical point of view, the differences introduced by the presence of subgrid terms in the underresolved simulations of hypersonic jets.

2. Flow configuration

We have studied numerically, and in Cartesian geometry, the temporal evolution of a 3D jet subject to periodicity conditions along the longitudinal direction. The flow is governed by the ideal fluid equations for mass, momentum, and energy conservation. In the astrophysical context, this formulation is usually considered to approximate the temporal evolution inside a spatial window of interstellar jets, which are highly compressible collimated jets characterized by Reynolds numbers of the order 10^{13-15}. It is known that the numerical solution of a system of ideal conservation laws (such as the Euler equations) produces the exact solution of another modified system with additional diffusion terms. With the discretizations used in this study it possible to verify *a posteriori* that the numerical viscosity implies an actual Reynolds number of about 10^3. In such a situation it is clear that the addition of the diffusive-dissipative terms into the governing equations would be meaningless. The formulation used is thus the following:

$$\frac{\partial \rho}{\partial t} + \frac{\partial}{\partial x_i}\left(\rho u_i\right) = 0 \tag{2}$$

$$\frac{\partial(\rho u_k)}{\partial t} + \frac{\partial}{\partial x_i}\left(\rho u_i u_k + p\delta_{ik}\right) = \frac{\partial}{\partial x_i} H\left(f_{\text{LES}} - t_\omega\right)\tau_{ik}^{SGS} \tag{3}$$

$$\frac{\partial E}{\partial t} + \frac{\partial}{\partial x_i}\left[(E+p)u_i\right] = \frac{\partial}{\partial x_i} H(f_{\text{LES}} - t_\omega)q_i^{SGS} \tag{4}$$

3

where the fluid variables p, ρ and u_i and E are, as customary, the filtered pressure, density, velocity, and total energy respectively. Here τ_{ik}^{SGS} and q_i^{SGS} are the subgrid stress tensor and total enthalpy flow, respectively. Function $H(\cdot)$ is the Heaviside step function, thus the subgrid scale fluxes are applied only in the regions where $f > t_\omega$. The threshold t_ω is here taken equal to 0.4, which is the value for which the maximum difference between the probability density function $p(f > t_\omega)$ between the filtered and unfiltered turbulence was observed [1]. Sensor f (1) is independent from the subgrid model used and from the kind of discretization used to actually solve the filtered transport equation, so that any subgrid model can be used. We have chosen to implement the standard Smagorinsky model as subgrid model,

$$\tau_{ij}^{SGS} + \frac{1}{3}\tau_{kk}^{SGS} = \rho\nu_\delta S_{ij}, \ \ \nu_\delta = (C_s\delta)^2 \mid S \mid$$

where S_{ij} is the rate of strain tensor and $\mid S \mid$ its norm. Constant C_s has been set equal to 0.1, which is the standard value used in the LES of shear flows, and the turbulent Prandtl number is taken equal to 1. The initial flow configuration is an axially symmetric cylindrical jet in a parallelepiped domain, described by a cartesian coordinate system (x, y, z). The initial jet velocity is along the y-direction; its symmetry axis is defined by $(x = 0, \ z = 0)$. The interface between the jet and the surrounding ambient medium is described by a smooth velocity and density transition in order to avoid the spurious oscillations that can be introduced by a sharp discontinuity. The flow profile is thus initialized as

$$\overline{u}(r) = \frac{U_0}{\cosh(r/a)^m}$$

where $r^2 = y^2 + z^2$ is the distance from the jet axis, a is the jet radius and U_0 the jet velocity. m is a smoothing parameter which has been set equal to 4. The same smoothing has been used for the initial density distribution,

$$\overline{\rho}(r) = \rho_0 \left(\nu - \frac{\nu - 1}{\cosh(r/a)^m} \right)$$

where ρ_0 is the density of the external ambient and ν is the ratio between the jet density and ρ_0. A value of ν larger than one implies that the jet is lighter than the external medium. The mean pressure is set to a uniform value p_0, that is, we are considering a situation where there is initially a pressure equilibrium between the jet and the surrounding environment. This initial mean profile

4

is perturbed at $t = 0$ by adding longitudinal transversal velocity disturbances whose amplitude is 1% of the jet velocity and whose wavelength is up to eight times the fundamental wavelength $2\pi/L$,

$$u_i(x,y,z) = \frac{1}{100}U_0 \sum_{n=0}^{8} \sin\left(n\frac{2\pi}{L}y + \varphi_n\right)$$

The integration domain is $0 \le x \le L -R \le y \le R, -R \le z \le R$, with $L = 10\pi a$ and $R = 6a$. We have used periodic boundary conditions in the longitudinal x direction, while zero normal derivative outflow conditions are used for all variables in the other directions. A scheme of the flow configuration used in the simulations is shown in figure 1.

In the following, all data have been made dimensionless by expressing lengths in units of the initial jet radius a, times in units of the sound crossing time of the radius a/c_0, where $c_0 = \sqrt{\gamma p_0/\rho_0})$ is the reference sound velocity of the initial conditions, velocities in units of c_0 (thus coinciding with the initial Mach number), densities in units of ρ_0 and pressures in units of p_0.

Equations (2-4) have been solved using an extension of the PLUTO code [6], which is a Godunov-type code that supplies a series of high-resolution shock-capturing schemes that are particularly suitable for the present application. The code has been extended by adding the subgrid fluxes and the computation of the functional f which allows to perform the selective large-eddy simulation. For this application, we chose a version of the Piecewise-Parabolic-Method (PPM), which is third order accurate in space and second order in time [13].

We have performed three simulations of a jet with an initial Mach number equal to 5 and a density ratio ν equal to 10. The density ratio is an important parameter in such flow configuration, as it has been shown that it has a strong influence on the time evolution and on the entrainment. The selective LES of the jet has been carried out on a 320×128^2 uniform grid. Moreover, two additional simulations were performed for comparison. A standard non selective LES where the subgrid model was introduced in the whole domain, which is obtained by putting $H \equiv 1$ in (2-4), and a higher resolution (640×256^2) Euler simulation obtained by putting $H \equiv 0$.

5

3. Results

In this jet configuration we can follow the evolution of a compressible jet from the amplification of its instable modes to its final quasi-steady state. As it is known form previous study on the subject (e.g.[4]), four main stages can be identified in the temporal evolution of hypersonic jet. In the first phase, the unstable modes exited by the perturbations grow up in accord to the linear theory, till their growth leads to the formation of internal shocks, then this stage is followed by a second phase where the jet is globally deformed and shocks are driven in the external medium, thus carrying momentum and energy away from the jet and transferring them to the external ambient. This is followed by a so called mixing stage: as a consequence of the shock evolution, mixing between the jet and external material begins to occur. The longitudinal momentum, initially concentrated inside the jet radius, is spread over a much larger region by the mixing of the jet material. In the end the jet reaches a statistically quasi-stationary phase and slowly decays.

The mixing phase where the flow can be considered turbulent, is reached after about 15 initial sound crossing times. At this point, the resolution could not be enough to solve all the scales and subgrid terms should start to be introduced in the underresolved regions. Figure 2 shows, in the selective large-eddy simulation, the probability that the sensor f is larger than the threshold, that is, that subgrid scales are present, at $t = 28$. At this stage about 40-60% of the jet is underresolved and there subgrid terms are applied. At the same time the external ambient is still resolved. The effect of the subgrid scale terms can be qualitatively appreciated in the visualizations of the pressure and density fields. A visualization of the pressure field in a longitudinal section at $t = 36$ is shown in figures 3(a-c) for the three simulations (selective LES, classical LES, high resolution Euler simulation). The comparison shows the higher smoothing and small scale suppression produced by the non selective use of the subgrid model. This is even more evident in the plot of the density field (figure 4): subgrid terms tend to delay the mixing of the jet and reduce the spreading of the jet material. The time evolution of the enstrophy distribution at two time instants far from the initial one is shown in figure 5 as a function of the distance from the centre of the jet. While the agreement between the

enstrophy distribution obtained with the selective LES simulation and with the reference high resolution Euler simulation is fair, the non selective simulation damps out the vorticity magnitude in the center of the jet and in the outer part, and introduces a spurious accumulation in the intermediate radial region. As a results, the vorticity dynamics is highly modified. The overall effect is a delay in the formation of the turbulent structures, as it is evident when the spectrum of the turbulent kinetic energy is considered. Figure 6 shows the kinetic energy spectrum at $r = 2$, that is in the intermittent region between the jet core and the surrounding ambient. In the non selective LES, there is a much lower energy in the fluctuations in the first part of the simulation. Moreover, even after they are generated ($t = 28$ and 36) there is a significant concentration of energy in the low wavenumber region, which becomes even more pronounced in the later stages ($t = 36$). This is consistent with the higher level of enstrophy seen in figure 5 for the non selective LES at a similar distances from the centre of the jet. Thus, we can observe that the selective introduction of the subgrid model yields distributions much closer, with respect to the standard LES, to the distribution shows by the high resolution Euler simulation.

A quantitative comparison of the different modelling procedures in the overall flow features can be made by considering the mean quantities, in particular the velocity longitudinal distribution and the jet thickness. The mean velocity profiles are shown in figure 8 where it is possible to appreciate not only the different temporal decay of the axial velocity but also the different shape of the velocity profiles. The geometrical thickness δ, here defined as the distance from the jet axis where $\overline{u}/U_0 = 0.5$, shows a low sensibility to how the flow is modelled, the vorticity thickness

$$\delta_\omega = \frac{U_0}{\max\left\{\frac{\mathrm{d}\overline{u}}{\mathrm{d}r}\right\}}$$

clearly indicates the delay in the growth and the higher collimation of the standard LES, where the reduced amount of turbulent kinetic energy reduces the spreading of the jet. The temporal growth rate can be transformed in an equivalent spatial growth rate by means of the Taylor transformation $x = U_0 t$, that is,

$$\frac{\mathrm{d}\delta}{\mathrm{d}x} = \frac{1}{U_0}\frac{\mathrm{d}\delta}{\mathrm{d}t}.$$

7

Both the higher resolution simulation and the selective LES present, in the second part of the simulation, an equivalent spatial growth rate equal to about 0.028. Such value is in line with what can be expected in such a flow [1].

4. Concluding remarks

In this work we have shown that the *selective* LES, which is based on the use of a scalar probe function f – a function of the magnitude of the local stretching-twisting operator – can be conveniently applied to the simulation of compressible jets. The probe function f was coupled with the standard Smagorinsky subgrid model. However, it should be noted that the use of f can be coupled with any model because f simply acts as an independent switch for the introduction of a subgrid model. The comparison among the three kinds of simulation (selective LES, standard LES, high resolution reference) here carried out shows that this method can improve the dynamical properties of the simulated field, in particular, the spectral distribution of the fluctuations over the resolved scales.

References

[1] D.Tordella, M.Iovieno, S.Massaglia, "Small scale localization in turbulent flows. A priori tests applied to a possible Large Eddy Simulation of compressible turbulent flows", *Comp. Phys. Comm.* **176**(8), 539-549 (2007).

[2] L.Biferale, G.Boffetta, A.Celani, A.Lanotte, F.Toschi, "Particle trapping in three-dimensional fully developed turbulence", *Phys. Fluids.* **17**(2), 021701/1-4 (2005).

[3] G.Bodo, P.Rossi, S.Massaglia, "Three-dimensional simulations of jets ", *Astron. & Astrophys.* **333**, 1117-1129 (1998).

[4] M. Micono, G. Bodo, S. Massaglia, P. Rossi, A. Ferrari, R. Rosner, "Kelvin-Helmholtz Instabilities in Three Dimensional Radiative Jets", *Astron. & Astrophys.*, **360**, 795-808 (2000).

[5] M.V.Morkovin, "Effects of compressibility on turbulent flows", in *Mècanique de la turbulence*, edited by A. Favre, 367, (1961).

[6] A.Mignone, G.Bodo , S.Massaglia, T.Matsakos, O.Tesileanu, C.Zanni and A.Ferrari, "PLUTO: a numerical code for computational astrophysics", *Astr. J. Supplement Series* **170**(1), 228-242 (2007), and http://plutocode.to.astro.it.

[7] M.Belan, D.Tordella, S.De Ponte, "Highly underexpanded jets in the presence of a density jump between an ambient gas and a jet", *Phys. Rev. E* **82**, 026303-1/10, (2010).

[8] C.Pantano, S.Sarkar, "A study in compressibility effevts in the high-speed shear flows using direct simulations", *J.Fluid Mech.*,**451**, 329–371 (2002).

[9] S.Stolz,N.A.Adams,L.kleiser, "The approximate deconvolution model for the large-eddy simulation of compressible flows and its application to shock-turbulent boundary layer interaction", *Phys.Fluids* **10**, 2985–3001, (2001).

[10] "An eddy-viscosity subgrid-scale model for turbulence shear flow: algebraic theory and applications", *Phys. Fluids* **16**, 3670–3681, (2004).

[11] F.Ducros, V.Ferrand, F.Nicoud, C.Weber, D.Darraq, C.Gacherieu, T.Poinsot, "Large-eddy simulation of the high-turbulence interaction", *J. comp. Phys.* **150**, 199–238, (1999).

[12] G.L.Brown, A.Roshko, "On density effects and large structure in turbulent mixing layers", *J. fluid Mech.* **64**, 775–816, (1974).

[13] P.Colella, P.R.Woodward, "The piecewisw parabolic method (PPM) for gas-dynamical simulations, *J. comp. Phys.* **54**(1), 174–201, (1984).
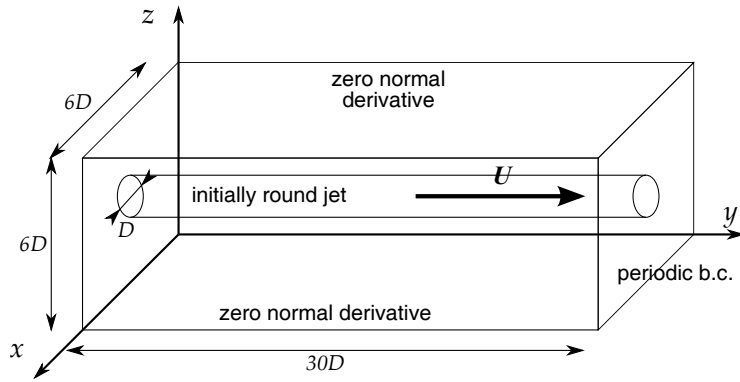
Figure 1: Scheme of the computational domain.
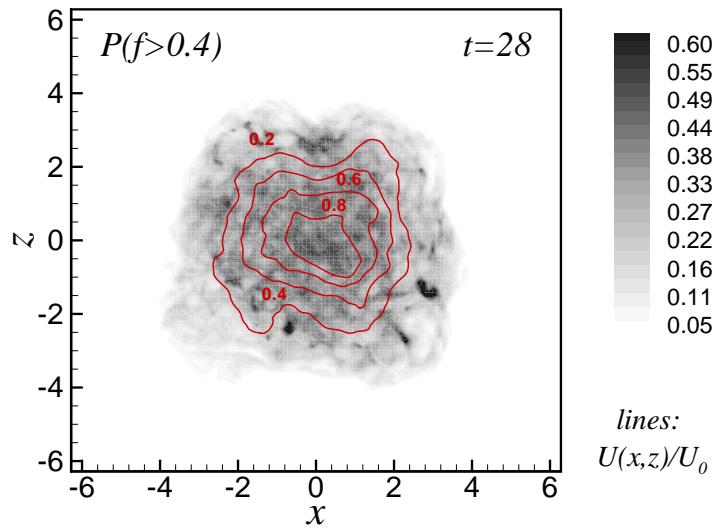
Figure 2: Contour plots of the probability that $f \geq t_\omega$ and thus that subgrid terms are introduced in the balance equation in the selective LES. The lines represent the levels of constant velocity $\overline{u}/U_0$, where U_0 is the jet axis velocity.
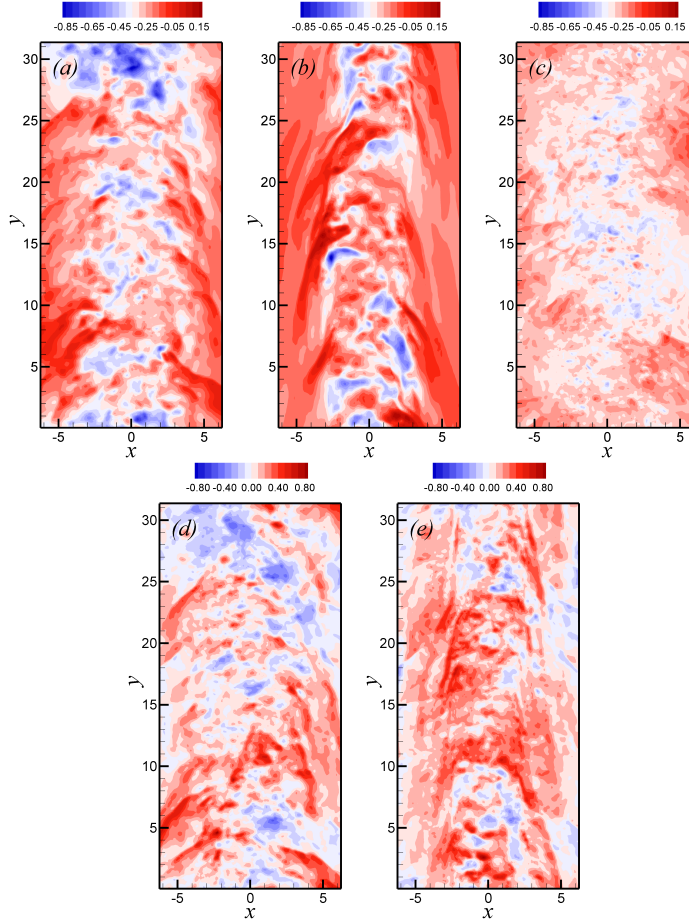
Figure 3: Pressure distribution in a longitudinal section at $t = 36$: (a) selective LES, (b) standard LES, (c) higher resolution pseudo-DNS. The figures show the contour levels of $\log_{10}(p/p_0)$, the mean flow is from bottom to top. Local difference between the pressure LES pressure fields and the higher resolution pseudo-DNS at $t/\tau = 32$: (d) selective LES, (e) standard LES. The figures show the contour levels of $(p_{LES} - p_{DNS})/p_0$.
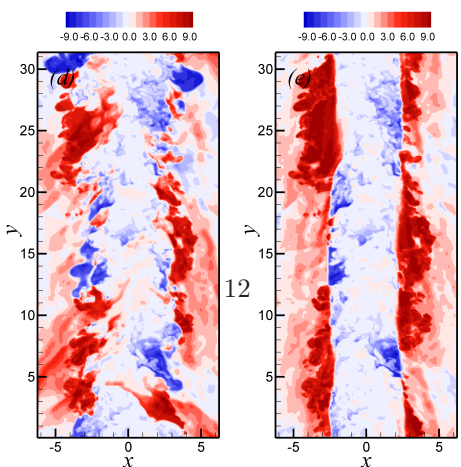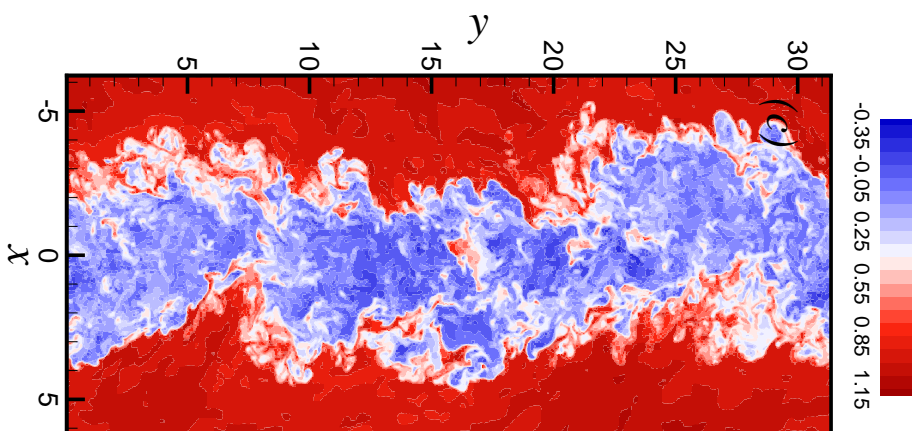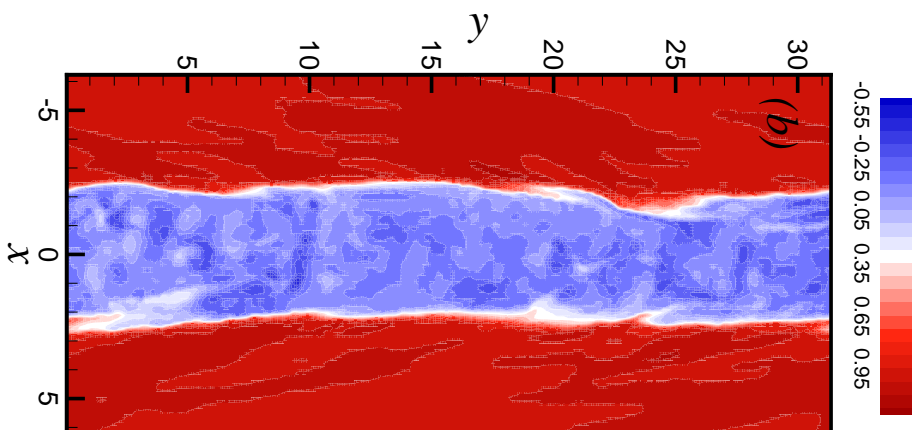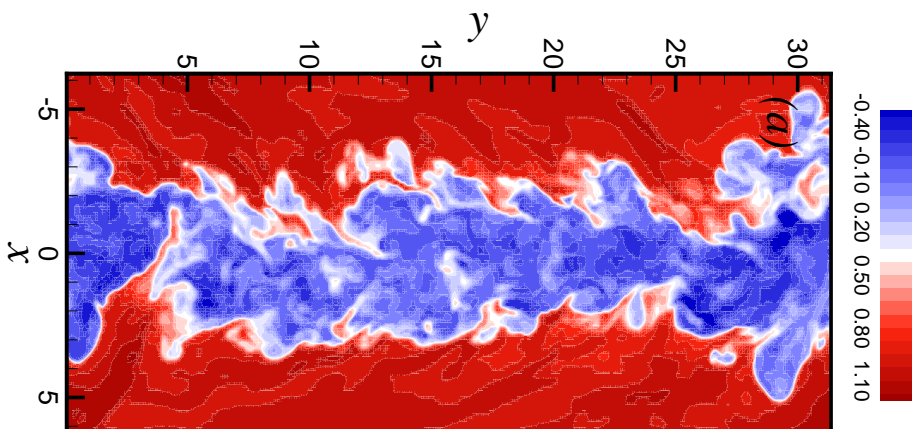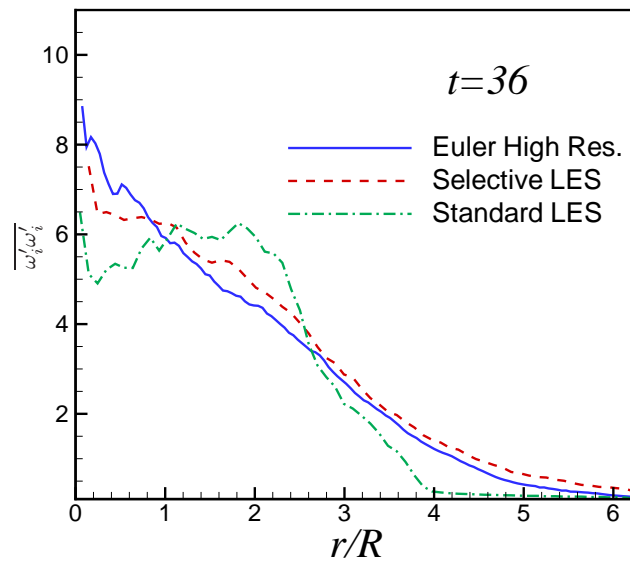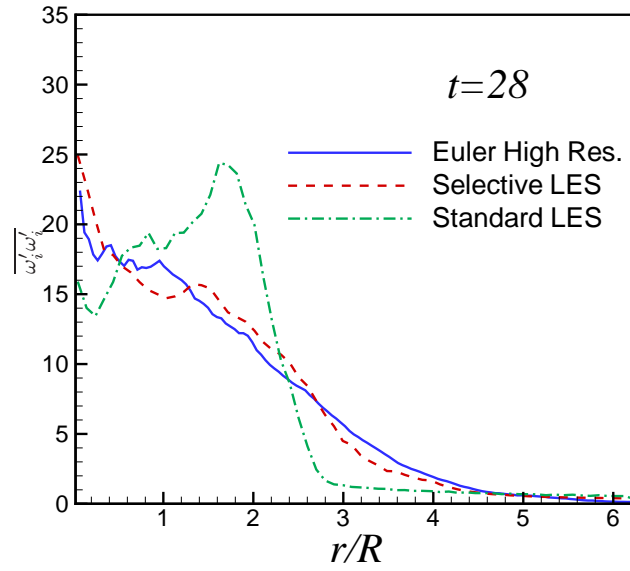
Figure 5: Radial distribution of the enstrophy, r is the distance from the axis of the jet. All averages have been computed as space averages on cylinders.
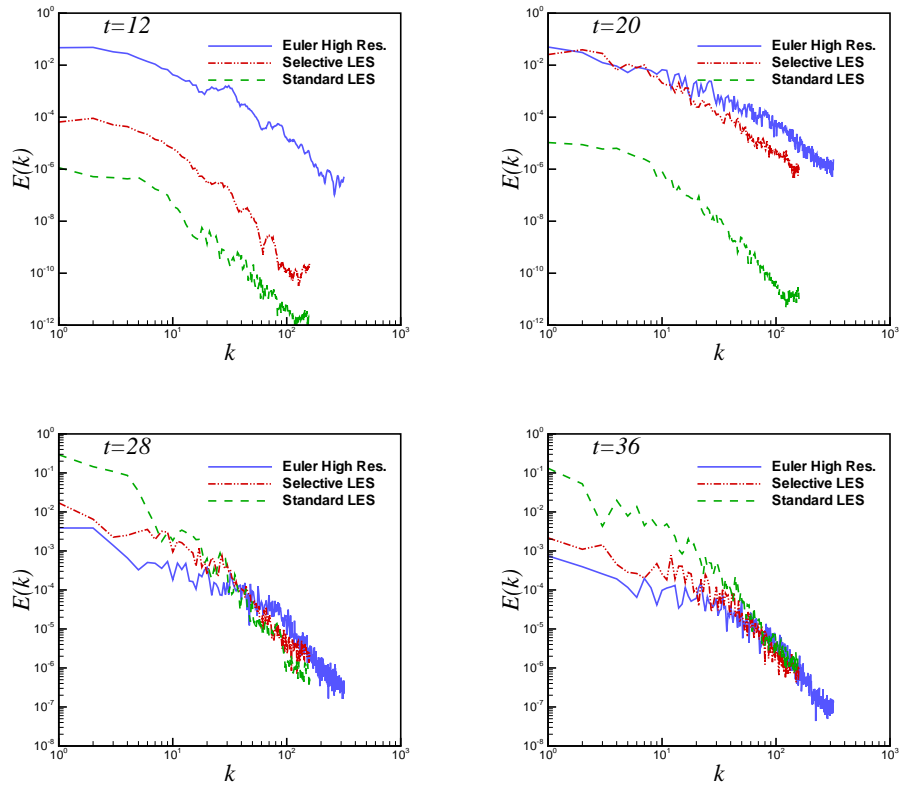
Figure 6: Spectra of the turbulent kinetic energy at $r = 2$, computed as the Fourier transform of the two-point correlations of the fluctuating kinetic energy $\rho u_i^2 / 2$.
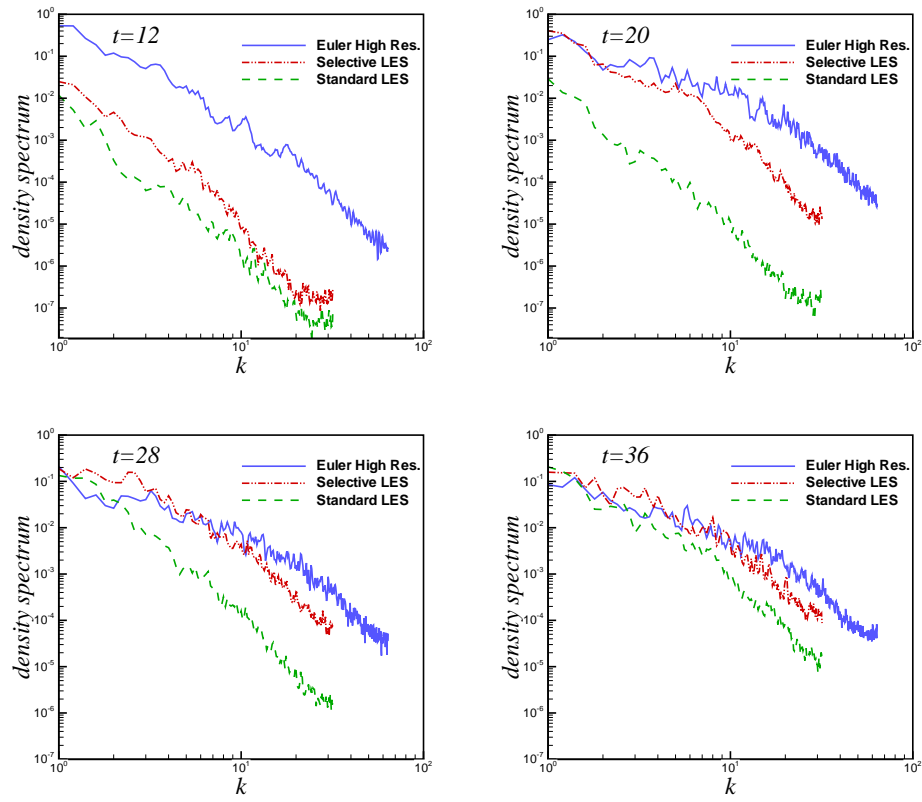
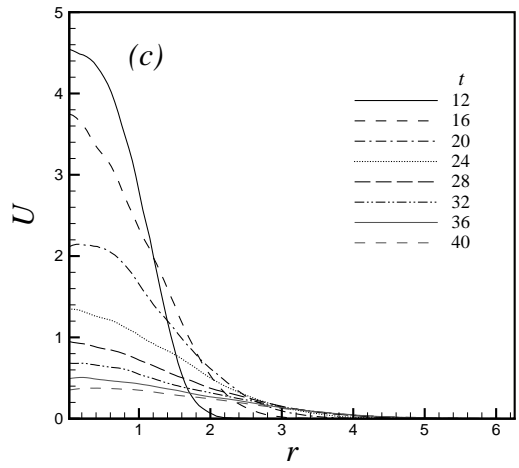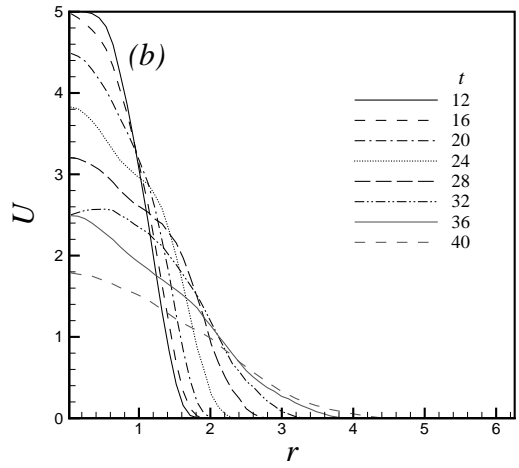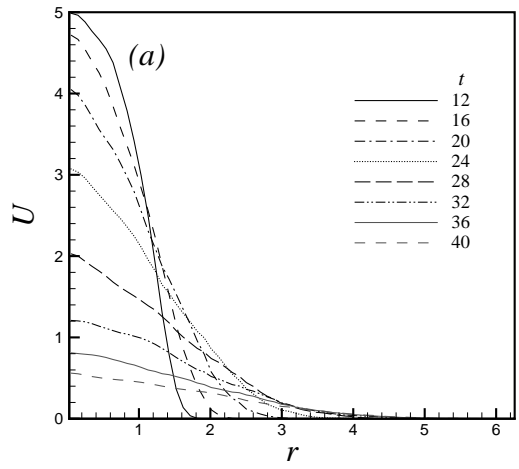Figure 7: Spectra of the density fluctuations at a distance from the jet axis equal to $r = 2$.

Figure 8: Mean longitudinal velocity profiles: (a) selective LES; (b) standard LES; (c) high resolution simulation.
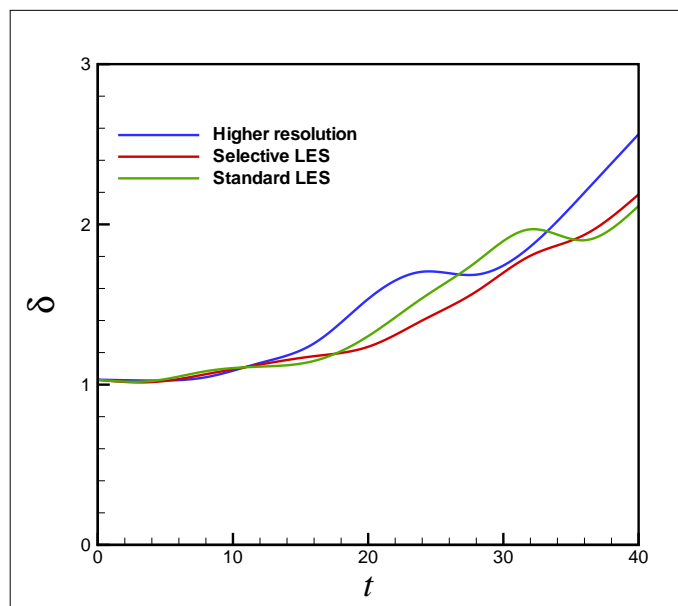
Figure 9: Time evolution of the geometrical thickness of the jet, evaluated as the distance from the jet axis where U/U_0 is equal to 0.5.
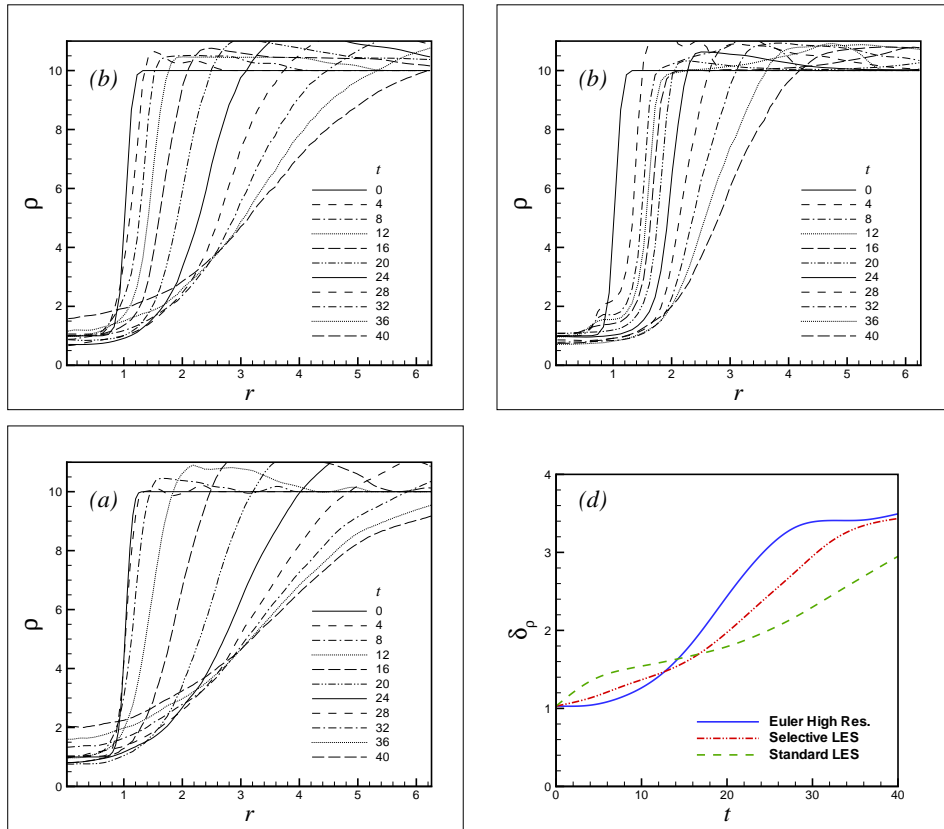
Figure 10: Time evolution of the mean density profiles and density thickness: (a) mean density, selective LES; (b) mean density, standard LES; (c) mean density, high resolution simulation, (d) density thickness δ_ρ.